JOURNAL OF VIROLOGY, Sept. 2009, p. 9195–9205 Vol. 83, No. 18
0022-538X/09/$08.00+0 doi:10.1128/JVI.00271-09

Protein Kinase G Phosphorylates Mosquito-Borne Flavivirus NS5▽

Dipankar Bhattacharya,[1]# Mayuri,[2]#† S. M. Best,[4] R. Perera,[2] R. J. Kuhn,[2] and Rob Striker[1,3]*

University of Wisconsin—Madison, Department of Medicine, Madison, Wisconsin 53706[1]; Purdue University, Department of Biological Sciences, West Lafayette, Indiana 47907[2]; W. S. Middleton Memorial Veterans Administration Hospital, Madison, Wisconsin 53706[3]; and Laboratory of Virology, Rocky Mountain Laboratories, National Institute of Allergy and Infectious Diseases, National Institutes of Health, Hamilton, Montana 59840[4]

Received 6 February 2009/Accepted 29 June 2009

Serine/threonine phosphorylation of the nonstructural protein 5 (NS5) is a conserved feature of flaviviruses, but the kinase(s) responsible and function(s) remain unknown. Mass spectrometry was used to compare the phosphorylation sites of the NS5 proteins of yellow fever virus (YFV) and dengue virus (DENV), two flaviviruses transmitted by mosquitoes. Seven DENV phosphopeptides were identified, but only one conserved phosphoacceptor site (threonine 449 in DENV) was identified in both viruses. This site is predicted to be a protein kinase G (PKG) recognition site and is a strictly conserved serine/threonine phosphoacceptor site in mosquito-borne flaviviruses. In contrast, in tick-borne flaviviruses, this residue is typically a histidine. A DENV replicon engineered to have the tick-specific histidine residue at this position is replication defective. We show that DENV NS5 purified from *Escherichia coli* is a substrate for PKG in vitro and facilitates the autophosphorylation of PKG as seen with cellular substrates. Phosphorylation in vitro by PKG also occurs at threonine 449. Activators and inhibitors of PKG modulate DENV replication in cell culture but not replication of the tick-borne langat virus. Collectively, these data argue that PKG mediates a conserved serine/threonine phosphorylation event specifically for flaviviruses spread by mosquitoes.

The flavivirus genus contains many medically important species, including dengue virus (DENV), yellow fever virus (YFV), West Nile virus (WNV), and tick-borne encephalitis virus (TBEV). More than 2 billion people are at risk of infection by DENV alone, leading to an estimated 50 million cases annually, which may increase further as the range of the mosquito vector expands with urbanization (24). While disease from mosquito-borne flaviviruses is particularly common, there are other flaviviral human pathogens that exist with transmission cycles that do not involve mosquitoes. Tick-borne transmission is the other well-described route, but non-arthropod-borne routes also exist (for example, bats). It is likely that each transmission route has genetic adaptations that facilitate that route, but such changes are not yet understood (7).

Serine/threonine phosphorylation is a conserved feature across all three genera of the family *Flaviviridae*, including the genus flavivirus (the others genera being pestivirus and hepacivirus). Among the features of *Flaviviridae*, the most-studied examples are the multiple phosphorylations of nonstructural protein 5A (NS5A) of hepatitis C virus, which exists in both basal (termed p56) and hyperphosphorylated (termed p58) states mediated by multiple kinases that both are necessary for and limit replication (14, 18, 23). Phosphorylation of NS5B, the RNA-dependent RNA polymerase (RdRP), has also been shown to affect replicon activity (10). In the genus flavivirus, several mosquito-borne viruses (DENV, WNV, and YFV) and at least one tick-borne encephalitis virus are known to have phosphorylated forms of nonstructural protein NS5 (2, 9, 11, 13, 19). In the genus flavivirus, NS5 is central to viral replication, as it possesses both RdRP and methyltransferase activities. DENV phosphorylation of NS5 correlates with the loss of NS5 interactions with the viral helicase NS3. A hyperphosphorylated form of NS5 was found to localize to the nucleus, away from the cytoplasmic sites of viral replication (6, 9). A nuclear localization sequence is present in DENV NS5 and is phosphorylated in vitro by host CKII, but the relationship between phosphorylation and nuclear localization has yet to be fully elucidated (17). Multiple different serine/threonine phosphorylation events likely occur in the flaviviral life cycle, potentially affecting various functions of NS5 (2), but the role of these events and identity of the kinase(s) responsible are largely unknown.

In this report, we used mass spectrometry to identify serine/threonine phosphorylation sites in DENV. A single phosphoacceptor site, previously identified in YFV, is conserved specifically in the mosquito-borne flaviviruses but not the tick-borne flaviviruses. Furthermore, in vitro studies reveal that this site is phosphorylated by a cyclic-nucleotide-dependent kinase, protein kinase G (PKG), and a phosphoacceptor threonine/serine is required for replication. Taken together, these data implicate the PKG pathway in flaviviral replication for the first time and suggest a host cell pathway that could be targeted by antiviral therapy.

MATERIALS AND METHODS

DENV-2 NS5 protein purification from *E. coli* and polymerase activity. The region encoding full-length NS5 (amino acid residues 1 to 900) of DENV-2 (GenBank accession no. U87411) was amplified using the DENV-2 cDNA as the template. The forward primer sequence for the full-length NS5 was 5′-TACTT CCAATCCAATGCCGGAACTGGCAACATAGGAGAGAC-3′, and the reverse primer sequence was 5′-TTATCCACTTCCAATGCTACCACAGAACT CCTGCTTCTTCC-3′. The amplified product was cloned into the expression

* Corresponding author. Mailing address: University of Wisconsin—Madison, Madison, WI 53706. Phone: (608) 262-2994. Fax: (608) 262-8418. E-mail: rtstriker@wisc.edu.

† Present address: Department of Biological Chemistry and Molecular Pharmacology, Harvard Medical School, Boston, MA 02115.

# These authors contributed equally.

▽ Published ahead of print on 8 July 2009.

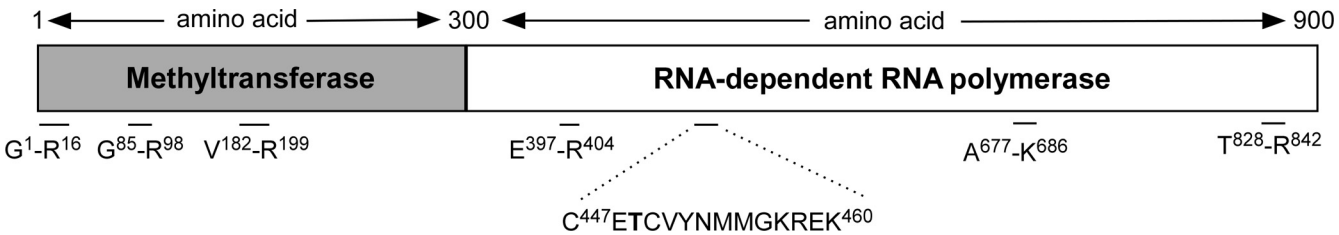

FIG. 1. Schematic of DENV NS5 phosphopeptides identified by MALDI-TOF analysis. Seven peptides were found to have a mass 80 Da greater than calculated when all residues were assumed to be unphosphorylated, and each lost 80 Da upon phosphatase treatment. The sequence of the peptide detailed in this study is given, and the threonine phosphorylated is in boldface.

vector pET30a by using ligation-independent cloning. The N-terminally His-tagged constructs for full-length DENV-2 NS5 were transformed into *Escherichia coli* expression strain BL21-Codon Plus (DE3)-RIL cells (Stratagene). Large-scale cultures (2 liters) for protein purification were grown in LB (supplemented with kanamycin and chloramphenicol), at 37°C, until the culture reached an optical density at 600 nm (OD_{600}) of 0.5. Protein expression was induced with IPTG (isopropyl-β-D-thiogalactopyranoside) at a final concentration of 0.4 mM. The induced culture was then grown for 6 h at 25°C. Cells were harvested by centrifugation at 6,000 × *g* for 10 min at 4°C and resuspended in lysis buffer containing 20 mM Na_2PO_4, pH 7.0, 0.5 M NaCl, 50 mM L-arginine, 50 mM L-glutamic acid, 10 mM $MgSO_4$, 5 mM imidazole, 5 mM β-mercaptoethanol, 1 mM phenylmethylsulfonyl fluoride, and 0.01 mg/ml (each) DNase I and RNase A. The cell suspension was lysed by sonication on ice, and the lysate was centrifuged at 25,000 × *g* for 30 min at 4°C. The supernatant was filtered through a 0.45-μm filter and subjected to immobilized metal affinity chromatography using a HisTrap HP column (GE Healthcare). The protein was eluted with 20 mM Na_2PO_4 buffer, pH 7.0, containing 0.5 M NaCl and 300 mM imidazole. Protein-containing fractions were then pooled, dialyzed overnight against 50 mM Tris buffer, pH 8.0, with 500 mM NaCl, 5 mM β-mercaptoethanol, and 5% glycerol, and concentrated. The concentrated protein was applied onto a Superdex 200 gel filtration column preequilibrated with the dialysis buffer. Fractions containing the full-length NS5 were pooled, and the protein was concentrated using a Vivaspin 30-kDa-molecular-mass-cutoff centrifugal concentrator (Vivascience). The purified protein was tested for in vitro RdRP activity as described in reference 21, with and without cyclic GMP (cGMP).

DENV-2 NS5 mutagenesis, RNA transcription, transfection, and replication analysis. A DENV-2 replicon cDNA (K. Combs, R. Perera, J. Smit, and R. J. Kuhn, unpublished results) was used to introduce mutations at position T449 of NS5. The replicon construct consisted of the DENV-2 genomic cDNA in which the genes encoding structural proteins were replaced by a *Renilla* luciferase reporter gene. Mutations T449S, T449H, and T449E were introduced into the DENV replicon cDNA by standard overlap PCR mutagenesis procedures (8). RNA transcripts of DENV-2 replicon were generated by in vitro transcription using T7 RNA polymerase (Amersham Biosciences) from DNA templates linearized by digestion with XbaI restriction enzyme in the presence of the $m^7G(5')ppp(5')G$ cap analog (NEB). HEK293T cells in a 24-well plate were transfected with 0.8 μg of purified RNA per well by using the Lipofectamine reagent (Invitrogen) according to manufacturer's instructions. A control replicon construct with NS5 catalytic aspartate residue deletions was transfected in parallel as a negative control. At 3, 6, 12, 24, 48, 72, 96, and 120 h posttransfection, the medium was removed and cells were washed with phosphate-buffered saline and lysed with 100 μl of 1× *Renilla* lysis buffer from the *Renilla* Luciferase Assay System (Promega, Madison, WI). The lysates were stored at −80°C. Prior to the assay, frozen extracts were thawed and then homogenized by briefly being subjected to a vortex. Luciferase activity was initiated by the addition of 10 μl of cytoplasmic extracts to 50 μl of *Renilla* luciferase substrate. Luciferase activity was detected using a Turner Designs TD20/20 luminometer and measured in relative light units.

YFV and DENV NS5-IRES-GFP constructs. The full length of either YFV NS5 (vaccine strain; GenBank accession no. X03700) or DENV NS5 (dengue type 2; GenBank accession no. M19197) was amplified from a DNA template by PCR with primers that introduce an XhoI site, Kozak sequences, an in-frame start codon (ATG) 5′ to the NS5 sequence, and a PacI site, as well as six-His codons in frame and a stop codon at the 3′ end. The ~2.8-kb PCR product was digested and cloned into the pIRES/GFP bicistronic mammalian expression vector (provided by Kouacou V. Konan, Penn State University, University Park, PA) in XhoI-PacI sites and sequenced. YFV NS5 T450A was generated by an overlap PCR strategy (8) with an introduction of threonine-to-alanine mutations in overlapping primer pairs. Second-step PCR products were directly cloned into a wild-type YFV NS5 six-His-tagged internal ribosome entry site (IRES)-green fluorescent protein (GFP) construct by replacing the Bsu36I-AvrII fragment and sequenced.

Expression and purification of YFV NS5 and DENV NS5 proteins in HEK293T cells. GFP in the IRES vector was used as a transfection/expression marker. Transfection of the empty vector was performed in parallel in each case as a negative control. Fifteen micrograms of YFV NS5 DNA, DENV NS5 DNA, or empty vector DNA was transfected with a cocktail of TransIT-LT1 (MirusBio, Madison, WI) into a T-75 flask containing 70 to 80% confluent HEK293T cells and incubated for 48 h in Dulbecco's modified Eagle's medium (DMEM) supplemented with 10% fetal bovine serum (FBS) and 1× penicillin-streptomycin solution (Invitrogen, La Jolla, CA) at 37°C in a 5% CO_2 incubator. The procedures for transfection, expression, and purification of the six-His-tagged protein were described previously (2).

Mass spectrometry sample preparation, sample loading, and analysis. Six-His-tagged, purified, and NS5-immunoprecipitated proteins (from experimental, empty vector, and mock-infected controls) from HEK293T cells were electrophoresed in 10% sodium dodecyl sulfate-polyacrylamide gel electrophoresis (SDS-PAGE) gels. The gels were stained with GelCode Blue stain (Thermo Fisher Scientific, MA). An ~100-kDa band was excised from the gel. In-gel digestion was performed with trypsin (Trypsin Gold, mass spectrometry grade; Promega, Madison, WI), dephosphorylated with calf intestinal alkaline phosphatase (CIAP) if necessary, purified with OMIX C_{18} Zip-Tip column (Varian, Harbor City, CA), and run in both matrix-assisted laser desorption ionization (MALDI)–tandem time of flight (TOF) (Applied Biosystems, Foster City, CA) and Finnigan LTQ linear ion trap (Thermo Fisher Scientific, MA) mass spectrophotometers for liquid chromatography-tandem mass spectrometry LC-MS-MS as described elsewhere (2). For MALDI-TOF analysis, the mass spectra were collected from *m/z* values of 700 to 4,000, and preliminary analysis was performed with GPS Explorer software (Applied Biosystems, Foster City, CA). After performing a Mascot database (Matrix Science, London, United Kingdom) search and data comparison before and after CIAP treatment (for the wild type only), detailed matching of mass with peptide identification was performed with MS-Digest tools (Web-based software in Protein Prospector, version 4.27.1). Electrospray ionization (ESI) mass spectrometry was performed for LC-MS-MS analysis. ESI precursor ion scan mass spectra were obtained using the Finnigan LTQ linear ion trap mass spectrometer equipped with a nanoelectrospray ion source. A Zorbax 300SB-C18 nanoflow high-performance liquid chromatography (HPLC) column (150 mm by 75 μm; Agilent Technologies, Santa Clara, CA) was eluted with a linear gradient of water-acetonitrile in the presence of 0.1% formic acid at a flow rate of 0.2 μl/min. The remainder of the protocol was followed as described elsewhere (3), and full-scan spectra were recorded from *m/z* values of 200 to 2,000 followed by the recording of MS-MS spectra in Xcalibur software (Thermo Fisher Scientific, MA). MS-MS spectra of detected phosphopeptides were searched against the FASTA database by using the Sequest search program within BioWorks Rev3.3 software (Thermo Fisher Scientific, MA).

In vitro phosphorylation of DENV NS5 by PKG. In vitro protein phosphorylation assays were performed by incubating 1 μg of bacterially expressed full-length six-His-tagged DENV NS5 protein with 5 μCi of [γ-^{32}P]ATP (Perkin Elmer, Waltham, MA), in the presence or absence of 10 μM cGMP (Calbiochem, Gibbstown, NJ) and 0.1 μg bovine lung PKG Iα (Calbiochem, Gibbstown, NJ) in kinase reaction buffer containing 0.2 mM EDTA, 20 mM HEPES (pH 7.5), 10 mM magnesium acetate, and 0.1 mM ATP containing 1× Halt phosphatase inhibitor cocktail (Thermo Fisher Scientific, Waltham, MA) in a total reaction volume of 25 μl. Prior to its addition to the reaction mixture, 5 μl of

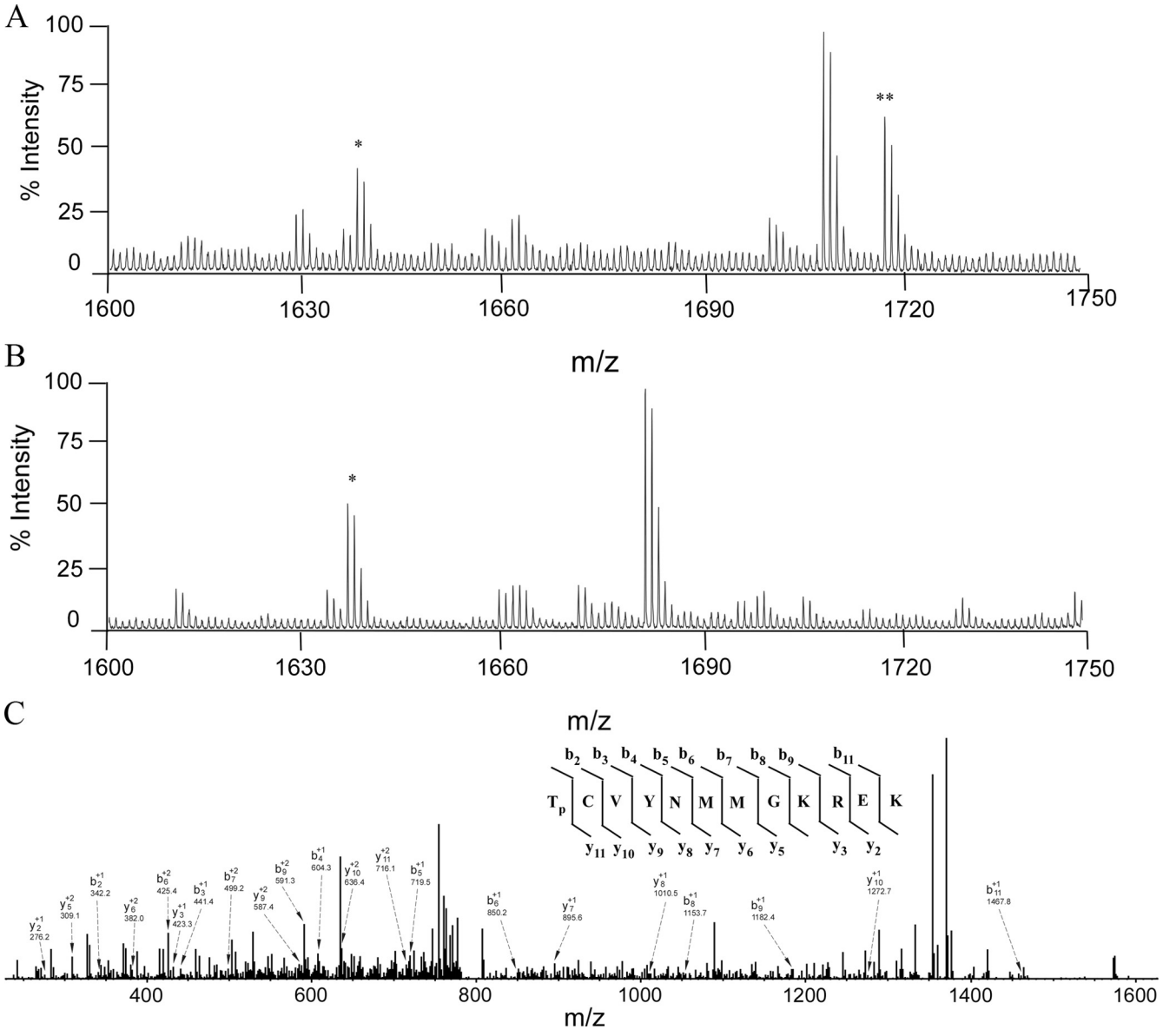

FIG. 2. Mass spectrometric analysis of wild-type YFV NS5 peptides generated by trypsin digestion after expression in HEK293T cells. The *m/z* was calculated for posttranslational modifications with additions of 15.9 for oxidation of each methionine and 57.02 for alkylation of each cysteine during in-gel digestion. (A) MALDI-TOF spectra of a singly charged monoisotopic peak of the peptides. A single asterisk indicates the unphosphorylated peptide corresponding to amino acids C^{448}RTCVYNMMGKR^{459}, with an *m/z* of 1,636.9243. Double asterisks indicate the same peptide in a phosphorylated form, with an increased *m/z* of 1,716.9217. The phosphopeptide *m/z* was calculated with an addition of 79.9 for one phosphate in the T^{450} position in the peptide sequences. (B) MALDI-TOF spectra of a singly charged monoisotopic peak of the peptides. The graph shows data for the phosphopeptides treated with 20 U of CIAP to remove phosphate, showing a complete loss of the phosphorylation peak (1,716.9217) present in panel A. A single asterisk indicates a dephosphorylated/unphosphorylated peak of C^{448}RTCVYNMMGKR^{459} of the CIAP-treated peptide with an *m/z* of 1,636.8253. (C) LC-MS-MS ionizations of the phosphorylated peptide corresponding to amino acids T^{450}CVYNMMGK REK^{461} after an in-gel digest by trypsin. The peptide was passed through a C_{18} HPLC column before fragmentation. Major fragment ions are labeled with their corresponding b (C-terminal) and y (N-terminal) ions and their charge states.

the supplied PKG stock solution was diluted in 8 μl of PKG dilution buffer containing 10 mM HEPES (pH 7.5), 1 mM EDTA, 6 mM dithiothreitol, 1 mg/ml bovine serum albumin, and 1x Halt protease inhibitor cocktail (Thermo Fisher Scientific, Waltham, MA). The reaction mixtures were incubated at 30°C for 15 min and terminated by adding Laemmli sample buffer in the reaction mixture, boiled for 3 min, and run in 10% SDS-PAGE. After the gel was dried, incorporated ^{32}P was detected by exposure of the gel to Kodak BioMax XAR film (Perkin Elmer, Waltham, MA) for 12 h at −80°C. The same gel was rehydrated in water for 1 h and stained with Coomassie blue to serve as a protein loading control.

Mass spectrometric analysis of in vitro-phosphorylated DENV NS5 by PKG. For mass spectrometry analysis of the in vitro kinase assay, the same protocol as described above was followed except that 0.2 mM nonradioactive ATP was used instead of [γ-^{32}P]ATP and the reaction mixture was incubated for 1 h at 30°C. After a staining with GelCode Blue solution (Thermo Fisher Scientific, Waltham, MA), the band of interest was excised from the gel, alkylated, in-gel digested with trypsin, further purified with OMIX C_{18} Zip-Tip column, and run in both MALDI-TOF and ESI analyses as described previously (2).

PKG inhibition and activation studies on viral yield. Small interfering RNA (siRNA) for PKG Iα/β, scrambled control siRNA, anti-PKG Iα antibody

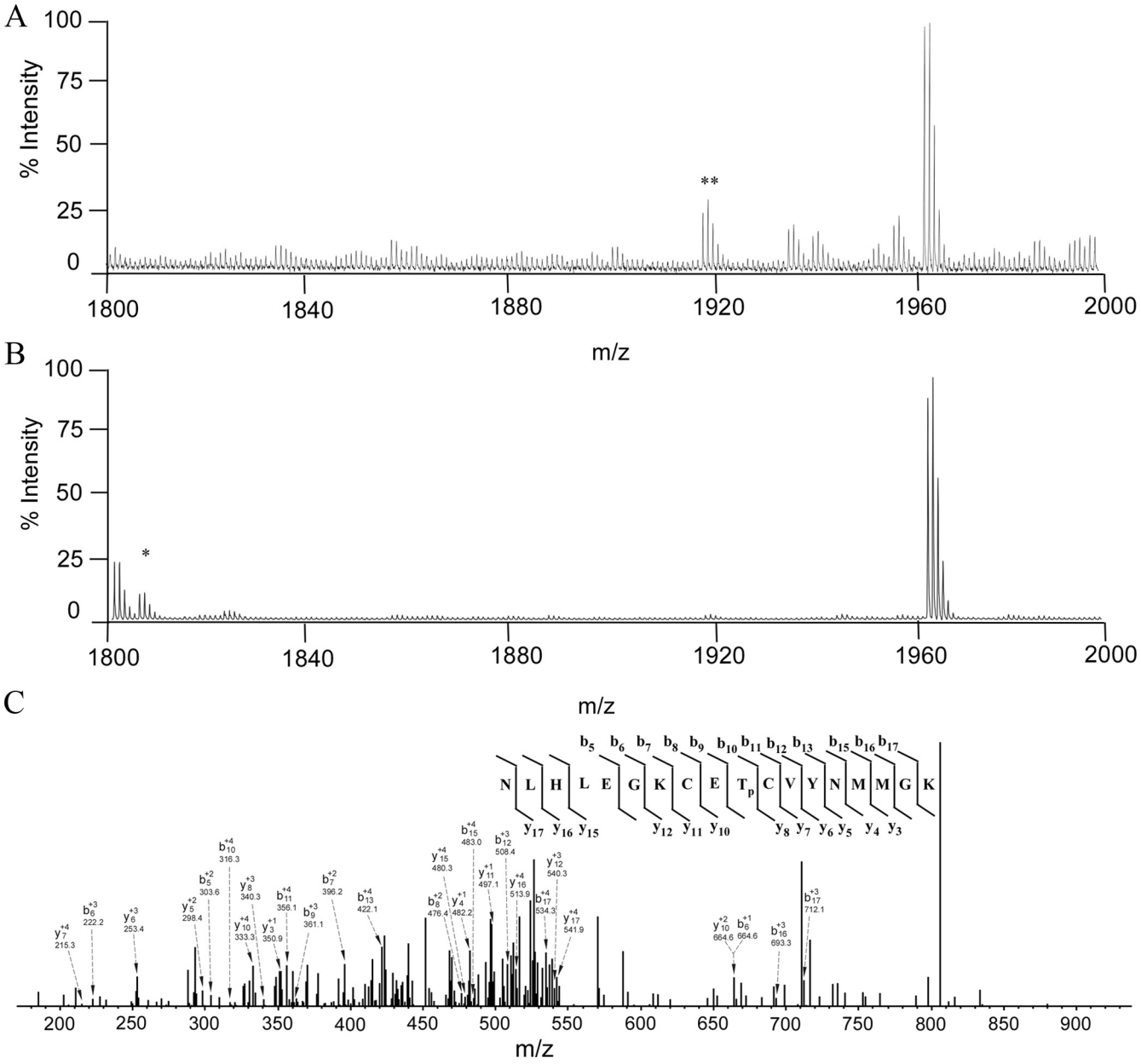

FIG. 3. Mass spectrometric analysis of DENV NS5 peptides generated by trypsin digestion after expression in HEK293T cells. (A) MALDI-TOF spectra of a singly charged monoisotopic peak of the peptides. Double asterisks indicate the phosphorylated peptide corresponding to amino acids $C^{447}ET_pCVYNMMGKREK^{460}$, with an *m/z* of 1,919.8923. The *m/z* was calculated for posttranslational modifications with additions of 15.9 for oxidation of methionine, 57.02 for alkylation of cysteine during in-gel digestion, and 79.9 for one phosphate in the T^{449} position. (B) MALDI-TOF spectra of the phosphopeptides treated with 20 U of CIAP to remove phosphate, showing complete loss of the phosphorylated peak (1,919.8923) present in panel A. A single asterisk indicates the dephosphorylated/unphosphorylated peak of $C^{447}ETCVYNMMGKREK^{460}$ of the CIAP-treated peptide with an *m/z* of 1,807.9477. This *m/z* was calculated with an addition of 57.02 for alkylation of cysteine. (C) LC-MS-MS ionizations of the phosphorylated peptide corresponding to amino acids $N^{440}LHLEGKCETCVYNMMGK^{457}$ after in-gel digest by trypsin. The peptide was passed through a C_{18} HPLC column before fragmentations. Major fragment ions are labeled with their corresponding b (C-terminal) and y (N-terminal) ions and their charge states. The *m/z* values were calculated for posttranslational modifications with additions of 15.9 for oxidation of one methionine, 57.02 for alkylation of each cysteine during in-gel digestion, and 79.9 for one phosphate in the T^{449} position.

(Santa Cruz Biotechnology, Santa Cruz, CA), and a PKG activity assay (Cyclex; distributed by MBL International) were used according to the manufacturers' instructions. DENV-2 (GenBank accession no. U87411) and, independently, TBEV (langat virus [LGTV] wild-type strain TP21) were used to infect HEK293T cells at a multiplicity of infection of ~0.25. For pharmacologic manipulation experiments, immediately after infection, cells were treated with a cell-permeable activator of PKG, guanosine 3′,5′-cyclic monophosphate, β-phenyl-1, N_2-ethano-8-bromo-, sodium salt (8-Br-PET-cGMP, Na), or a cell-permeable inhibitor, guanosine 3′,5′-cyclic monophosphorothioate,8-(4-chlorophenylthio)-, Rp isomer, triethylammonium salt (Rp-8-pCPT-cGMPS, TEA) (Calbiochem, Gibbstown, NJ). For siRNA studies, cells were infected 48 h after transfection. Medium from infected cells was harvested at 48 h, and a focus-forming assay for DENV (16) or TBEV (12) was used to quantify the viral yield.

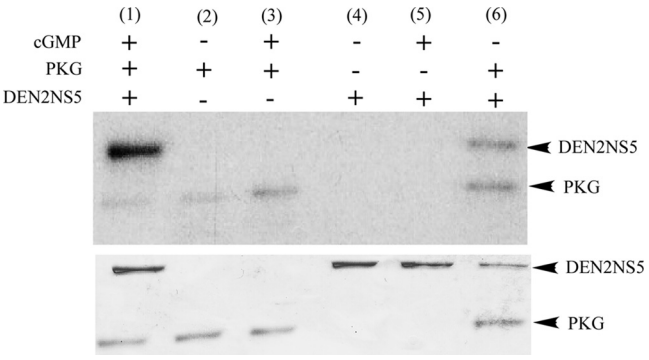

FIG. 4. PKG Iα can phosphorylate DENV NS5 in vitro. One microgram of the bacterially expressed six-His-tagged, purified full length of DENV NS5 (amino acid coordinate number G1-L901) was incubated in the presence or absence of 0.1 μg of bovine lung PKG Iα, 10 mM of cGMP, and [γ-^{32}P]ATP in an in vitro kinase assay. (Upper panel) The reaction mixture was separated by 10% SDS-PAGE, and incorporated ^{32}P was detected by autoradiography. DENV NS5 was highly phosphorylated in the presence of PKG Iα (lane 1), was less phosphorylated in the absence of cGMP (lane 6), and had no phosphorylation in the absence of PKG Iα (lanes 4 and 5). PKG was able to phosphorylate in the presence of DENV NS5 (lane 6) to a greater degree than it was able to autophosphorylate in the absence of DENV NS5 (lanes 2 and 3) substrate. (Lower panel) The same gel after Coomassie staining for protein loading.

Cytotoxicity assays. Cytotoxicity of the compounds that alter PKG activity was measured spectrophotometrically by monitoring the reduction of a tetrazolium salt to a formazan dye by mitochondrial dehydrogenase in living cells in the presence or absence of the compound. HEK293T cells were grown in DMEM, supplemented with 10% FBS in a 96-well plate at 37°C, and overlaid with culture media containing serial dilutions of the PKG inhibitor or activator (concentrations of 0.25 μM to 5 μM) or dimethyl sulfoxide (0.1% to 1%). Untreated cells served as positive controls. Cells were then incubated at 37°C in 5% CO_2 for ~48 h. The medium on cells was then replaced with 100 μl of WST-1 substrate from the Quick Cell proliferation kit (Biovision Inc., CA), diluted in DMEM and 2.5% FBS. Cells were incubated at 37°C for an additional 2 h. Plates were then removed, and the OD_{450} values were measured using a 96-well plate reader (Molecular Devices, Sunnyvale, CA). The OD_{450} values for cells treated with the compounds that alter PKG were compared to those obtained for cells treated with the dimethyl sulfoxide-treated or untreated controls to determine relative cytotoxicity.

Bioinformatics logo analysis. After alignment of 689 different full-length genomes from mosquito-borne flaviviruses and 26 tick-borne flaviviruses available through the Viral Bioinformatic Resource Center (www.biovirus.org), the logo analysis was performed using a Web-based program called WebLogo (5).

RESULTS

A conserved threonine residue is a phosphorylated site in YFV and DENV NS5. In a previous study, NS5 of YFV was purified from mammalian cells, and seven tryptic phosphopeptides were identified via MALDI; all seven had a mass 80 Da greater than predicted (2). All fragments lost 80 Da when exposed to CIAP, and these fragments represented at least six unique serine/threonine phosphorylation sites (2) (one site was represented twice, once by an incomplete tryptic digest). Here, we pursued a similar strategy and transfected HEK293T cells with a genetic construct that expresses six-His-tagged DENV NS5. The NS5 protein was purified using metal affinity chromatography, and the protein was excised from an SDS-PAGE gel. The products of both phosphatase-treated and untreated tryptic digests were compared. For both the YFV NS5 and the DENV NS5, peptides that cover over half of the total polypeptide (either at the calculated mass or 80 Da greater than the calculated mass) could be detected as ionized by the mass spectrometer. Therefore, many but not all of the conserved potential phosphorylated sites for both proteins could be compared. As in YFV, seven peptides whose mass was 80 Da greater than predicted and could be shifted to the predicted mass by phosphatase treatment were identified, but six of the sites were not identified previously (Fig. 1). Only one homologous peptide with an identical phosphorylation site in both YFV NS5 and DENV NS5 could be identified. Figure 2A shows the *m/z* of the YFV peptide C^{448}RTCVYNMMGKR^{459}, 1,636.9243, as well as the putative phosphorylated version of this peptide, with an *m/z* of 1,716.9217. Figure 2B shows that the higher-*m/z* peptide was lost after this preparation was treated with CIAP. Similar data were obtained for a smaller peptide, T^{450}CVYNMMGK^{458}, which also suggested that T450 was phosphorylated (data not shown). When a T450A mutant YFV NS5 construct was engineered, transfected into cells, and purified, neither the 1,636.9243 nor the 1,716.9217 *m/z* was detected (data not shown). Definitive evidence for phosphorylation at that particular site was provided by LC-MS-MS ionization of the mass shown in Fig. 2C. The homologous phosphorylated peptide $C^{447}ET_pCVYNMMGKREK^{460}$ (where the subscript "p" indicates that the T is phosphorylated) could also be identified when DENV NS5 was expressed in HEK293T cells (Fig. 3A). Treatment with CIAP led to the loss of this

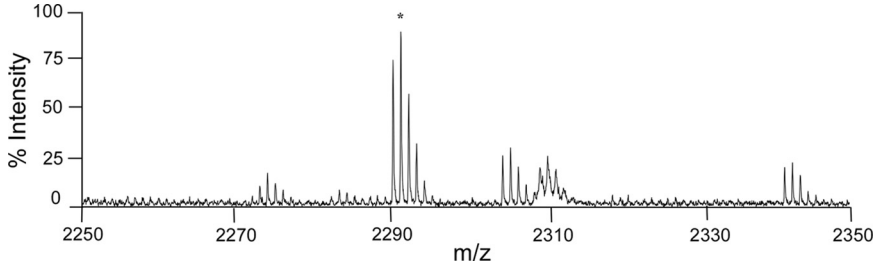

FIG. 5. MALDI-TOF analysis of in vitro-phosphorylated DENV NS5 generated by trypsin digestion and purified from *E. coli*. The six-His-tagged, purified full length of DENV NS5 (amino acid coordinate number G1-L901) was incubated in the presence of bovine lung PKG Iα, cGMP, and ATP in an in vitro kinase reaction. An ~100-kDa band of DENV NS5 was excised from SDS-PAGE gel, and after in-gel tryptic digestion, the phosphopeptides were detected by MALDI-TOF analysis. A single asterisk indicates the monoisotopic peak of the phosphorylated peptide corresponding to amino acids N^{440}LHLEGKCET$_p$CVYNMMGK^{557}, with an *m/z* of 2,291.9620. The phosphopeptide mass was calculated with an addition of 79.9 for one phosphate in the T^{449} position in the peptide sequences.

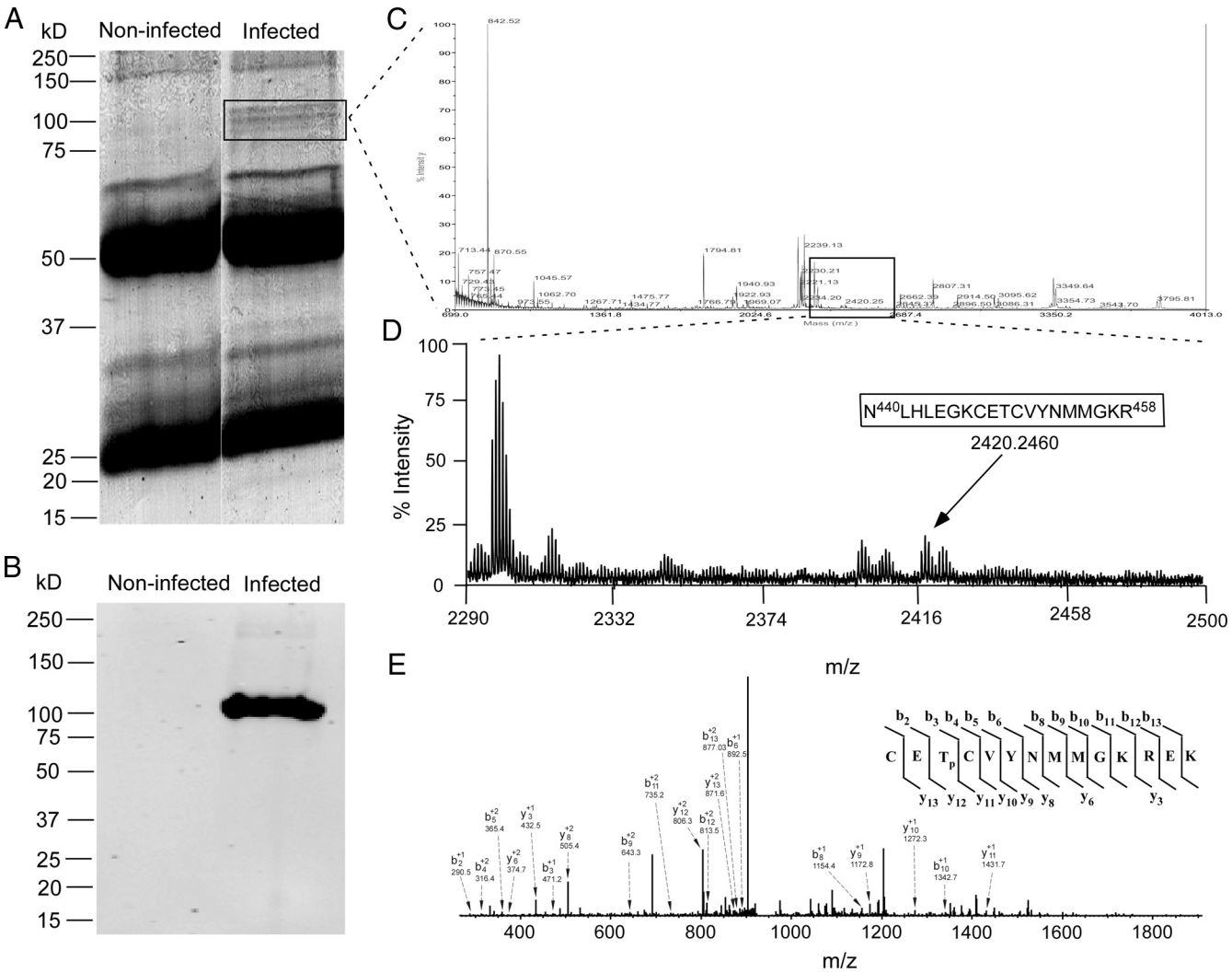

FIG. 6. DENV NS5 with phosphorylated T449 in infected HEK293T cells. (A) At 48 h postinfection, DENV NS5 was immunoprecipitated with an anti-NS5 antibody and identified in a 10% SDS-PAGE gel with a colloidal staining method. An ~100-kDa band corresponds to DENV NS5 in the infected-cell preparation lane and was completely absent in mock-infected cells. Three bands (boxed; likely representing a different phosphorylated form of DENV NS5) were excised from the gel and prepared for mass spectrometry analysis. (B) Western blot of the same preparation as in panel A with anti-DENV NS5 antibody indicating the position of DENV NS5 in an SDS-PAGE gel. (C) The MALDI-TOF analysis of full-scan spectra corresponds to a 100-kDa band of DENV NS5. (D) Enlarged view of the spectra that are boxed in panel C. The singly charged monoisotopic peak of single phosphorylated peptide corresponds to amino acids 440 to 458, with an *m/z* of 2,420.2460. The *m/z* was calculated for posttranslational modifications, with additions of 57.02 for alkylation of two cysteines during in-gel digestion and 79.9 for one phosphate. (E) LC-MS-MS ionizations of the phosphorylated peptide corresponding to amino acids C^{447}ETCVYNMMGKREK^{460} after in-gel tryptic digestion. The peptide was passed through a C_{18} HPLC column before fragmentations. Major fragment ions are labeled with their corresponding b (C-terminal) and y (N-terminal) ions and their charge states. The *m/z* was calculated for posttranslational modification with additions of 15.9 for oxidation of one methionine, 57.02 for alkylation of two cysteines during in-gel digestion, and 79.9 for one phosphate in the T^{449} position.

peak and detection of an *m/z* consistent with the unphosphorylated form (Fig. 3B). In the experiment involving YFV (Fig. 2), both phosphorylated and unphosphorylated versions of NS5 were detected in the sample not treated with CIAP, but in the DENV experiment, the unphosphorylated form was found only after CIAP treatment. Again, LC-MS-MS analysis of the phosphorylated peak revealed that this *m/z* corresponds to N^{440}LHLEGKCET$_p$CVYNMMGK^{457} (Fig. 3C). The threonine in this peptide corresponds to amino acid 449 instead of 450, as in the case of YFV NS5, due to a one-amino-acid insertion in the YFV methyltransferase domain relative to DENV NS5, yet the surrounding cysteines at both sites provide strong evidence that these two amino acids are structurally homologous.

DENV threonine 449 is phosphorylated by PKG in vitro. The threonine residue identified above as a phosphorylated site in both DENV and YFV NS5 proteins is also predicted to be phosphorylated by PKG via the neural net bioinformatics program (4). PKG kinases (isoforms Iα, Iβ, and II) are present in both mammals and insects. The PKGs regulate and are regulated by cGMP levels in the cell (20). Purified PKG Iα (bovine lung) was therefore used in vitro to phosphorylate

FIG. 7. Logo analysis of >700 flaviviral genomes separated by transmission vector. (A) Mosquito-borne flavivirus NS5 sequences were aligned, and logo analysis was performed by selecting 12 amino acids around the phosphorylation site of interest. The asterisk indicates position 449 in DENV or position 450 in YFV, which is highly conserved with either threonine (T) or serine (S), respectively, among all mosquito-borne flaviviruses. (B) Twenty-six tick-borne flavivirus NS5 sequences were aligned, and logo analysis was performed for the amino acids around the residue of interest (asterisk).

recombinant DENV NS5 purified from *E. coli* (unphosphorylated). [γ-^{32}P]ATP, PKG Iα, and DENV NS5 were incubated for 15 min at 30°C in the presence and absence of cGMP. In the presence of cGMP, DENV NS5 became phosphorylated (Fig. 4, lane 1, upper band). It is noteworthy that some degree of autophosphorylation of PKG was detected (Fig. 4, lane 1, lower band). This autophosphorylation is frequently modulated by cellular substrates of PKG and occurs at multiple sites (22). It occurred in the absence of DENV NS5 substrate (Fig. 4, lane 2) and was enhanced by the presence of cGMP (compare the lower bands in lane 2 and lane 3). In the absence of cGMP, DENV NS5 was still phosphorylated by PKG Iα, and again, autophosphorylation of PKG occurred (Fig. 4, lane 6). More autophosphorylation of PKG in the absence of cGMP occurred when DENV NS5 was present (Fig. 4, compare the lower bands in lane 6 and lane 2 in the top panel), whereas when cGMP was present, the opposite occurred (compare lower bands of lane 3 and lane 1). This suggested a complex interplay between the exogenous substrate (DENV NS5) and the PKG autophosphorylation sites that may be altered by cGMP, an allosteric activator of PKG. PKG Iβ (human) and PKG II (rat) also were able to phosphorylate DENV NS5 in vitro (data not shown). In vitro kinase reactions of DENV NS5 with PKG were then analyzed by mass spectrometry to determine if the same threonine was phosphorylated both in cells (shown in Fig. 1 and 2) and in vitro. A phosphorylation reaction involving PKG Iα, cGMP, and NS5 (Fig. 4, lane 1) was performed with nonradioactive ATP. The NS5 band was excised from an SDS-PAGE gel, digested with trypsin, and analyzed by MALDI-TOF analysis. A peak consistent with the *m*/*z* of the phosphorylated peptide was found (Fig. 5). Taken together, these data argue that the conserved CXTC motif (with X indicating R or E) is accessible both in vitro and in cells to be phosphorylated and can be phosphorylated by any of the members of the PKG family.

DENV NS5 residue 449 phosphorylation is detectable in infected cells. HEK293T cells were infected with DENV at a multiplicity of infection of 10, and cell lysates were harvested at 48 h. A polyclonal antibody specific to NS5 was used to immunoprecipitate NS5, which was then analyzed by SDS-PAGE. Three faint bands (Fig. 6A) not present in the immunoprecipitation lysate from mock-infected cells but detected by Western blotting with anti-NS5 antibody (Fig. 6B) were excised and trypsinized before being subjected to MALDI-TOF analysis (Applied Biosystems, Foster City, CA) (Fig. 6C and D). MS-MS revealed that residue 449 of DENV NS5 was phosphorylated (Fig. 6E).

The CXTC phosphoacceptor site is conserved specifically in the mosquito-borne lineage but not the tick-borne lineage of flaviviruses. Due to the conserved nature of the CXTC motif between YFV and DENV, we examined this motif throughout the genus. Using the Viral Bioinformatics Resource Center website (www.biovirus.org), we examined >700 full flaviviral genomes. Among viruses transmitted by mosquitoes, 689 different full genomes were available (several different isolates of DENV-1 to DENV-4, YFV, WNV, and Japanese encephalitis virus, among others), and for all of these, either a serine or threonine phosphoacceptor site was present in the protein (Fig. 7A). On the other hand, from the 26 available full genomes from viruses known to be transmitted by ticks, neither serine nor threonine was present at the relevant position; rather, a CXHC or CXQC motif was observed (Fig. 7B).

Replacement of Thr with His polymorphism from tick-borne flaviviruses rendered the DENV replicon nonfunctional. To determine the importance of Thr449, the DENV subgenomic replicon was engineered to replace the threonine in the CXTC motif with a serine, histidine, or a glutamic acid. The positively charged mutant histidine that naturally occurs in tick-borne viruses rendered the DENV replicon nonfunctional. Replacement of threonine with glutamic acid (a negatively charged residue which may mimic the effect of a nonreversible phosphorylation event) also significantly impaired DENV replicon replication (Fig. 8). However, the efficiency of replication from the DENV replicon containing the serine mutant was almost as high as that from the threonine-containing wild type.

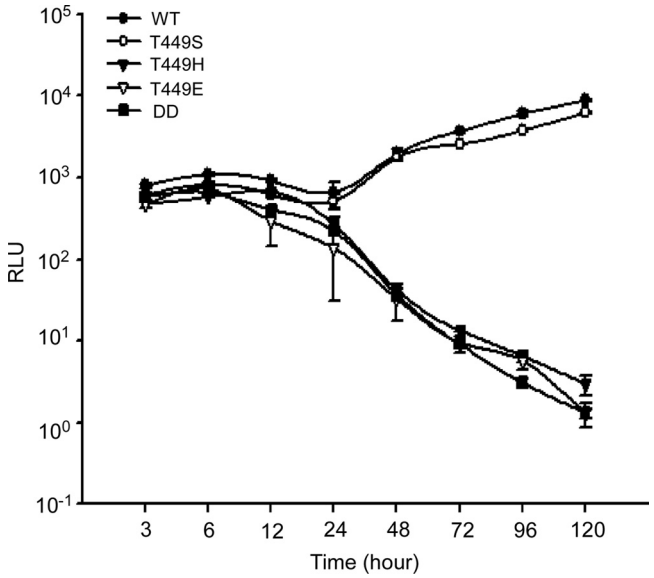

FIG. 8. Tick-specific histidine does not productively replace threonine 449 in the DENV replicon. The luciferase expression (relative light units [RLU]) from a wild-type (WT) DENV replicon after transfection was compared to replicons in which the position 449 residue was mutated to serine, glutamic acid, or histidine or a replicon with a polymerase-defective (DD) mutant.

Modulation of PKG levels alters DENV replication but not LGTV replication. We next examined if cell-permeable small molecules that either activate or inhibit PKG activity directly also modulate DENV replication. HEK293T cells were treated with various concentrations of a cell-permeable activator of PKG (8-Br-PET-cGMP, Na) (Fig. 9A) or a cell-permeable PKG inhibitor (Rp-8-pCPT-cGMPS, TEA) (Fig. 9B) before infection with DENV, and the yield of virus was measured by a focus-forming assay. Chemical activation and inhibition of PKG caused opposite and statistically significant changes to the DENV yield in the culture supernatant. Chemical activation of PKG activity resulted in viral production fourfold greater than the production without activation (*P* value, 0.0006). This is in contrast to the almost 10-fold inhibition of viral production when PKG was chemically inhibited relative to viral production without inhibition (*P* value, 0.00005). Neither drug exerted significant or observable cytotoxicity at these concentrations, as measured by an MTT [3-(4,5-dimethyl-2-thiazolyl)-2,5-diphenyl-2H-tetrazolium bromide] assay. No change in viral titers occurred when tick-borne-virus (LGTV)-infected HEK293T cells were treated with the same concentrations of the PKG activator (*P* value of 0.84 for the comparison of 0 μM to 5 μM; Fig. 9C) and the PKG inhibitor (*P* value, 0.96; Fig. 9D). We also utilized an siRNA approach to silence PKG in HEK293T cells to investigate if this resulted in a similar viral inhibition that was specific to DENV over LGTV. siRNA inhibition decreased both PKG Iα levels, according to

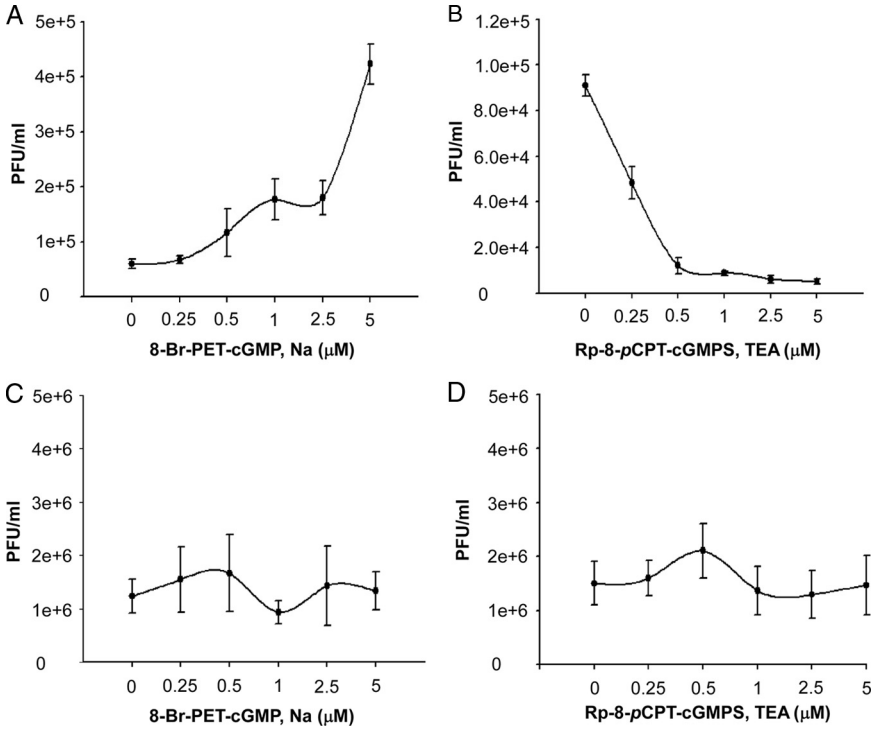

FIG. 9. Pharmacologic modulation of PKG activity in cells alters DENV replication but not TBEV replication. HEK293T cells were infected with either DENV strain 16681 or LGTV (TBEV) and treated with the indicated concentration of either PKG activator (8-Br-PET-cGMP, Na) (DENV [panel A]and TBEV [panel C]) or PKG inhibitor (Rp-8-pCPT-cGMPS, TEA) (DENV [panel B] and TBEV [panel D]). After 48 h, the media were harvested and the viral yield was quantified in a focus-forming assay in triplicate. Student's *t* test comparing the 5 μM condition to the 0 μM condition yielded *P* values of 0.0006 for panel A, 0.00005 for panel B, 0.84 for panel C, and 0.96 for panel D. FFU, focus-forming units.

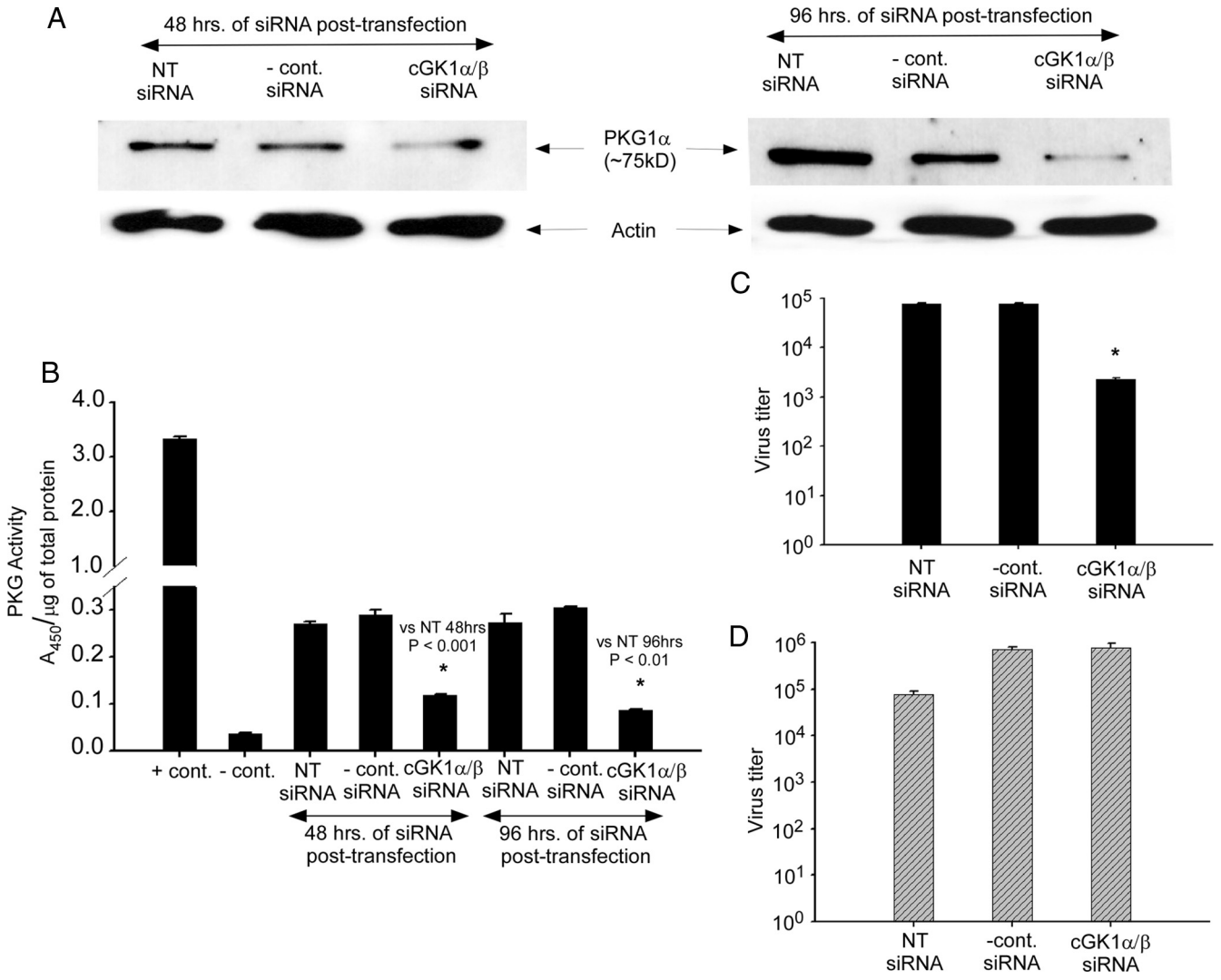

FIG. 10. RNA interference-mediated inhibition of PKG activity in cells inhibits DENV but not TBEV replication. PKG of HEK293T cells was silenced by transfecting 300 nM of a cGKIα/β siRNA pool for 96 h. Forty-eight hours after siRNA transfection, the cells were infected with either DENV strain 16681 or TBEV at a multiplicity of infection of 0.25. After 48 h of infection (96 h of siRNA posttransfection), the media were harvested and the viral yield was quantified in a focus-forming assay in triplicate three times. Non-siRNA-transfected cells were also prepared in parallel as positive controls. (A) Western blot with anti-cGKIα antibody shows the expression level of PKG Iα in HEK293T cells after silencing PKG Iα/β at 48 h and 96 h of posttransfection with either non-siRNA-transfected cells (NT siRNA), scrambled siRNA-transfected cells (−cont. siRNA), or cGKIα/β siRNA pool. The lower panel is the Western blot of the same respective blot with antiactin antibody demonstrating protein loading. (B) Comparison of PKG activities in between nontransfected, scrambled siRNA-transfected, and cGK1α/β siRNA-transfected HEK293T cells in total cell lysate after silencing PKG with an siRNA pool. About 60% of PKG activity was knocked down 48 h after transfection of the cGKIα/β siRNA pool, and more than 80% of PKG activity was knocked down 96 h after transfection of the cGKIα/β siRNA pool. Purified bovine PKG Iα (+cont) and buffer (−cont; no substrate) were used as positive and negative/background controls, respectively, when measuring PKG activity. (C) The bars represent the production of DENV in NT cells, scrambled siRNA-transfected cells, and PKG-silenced cells in a focus-forming assay. The viral yield was significantly decreased ($P < 0.00001$) in PKG-silenced cells. (D) The hatched gray bars represent the production of TBEV in NT cells, scrambled siRNA-transfected cells, and PKG-silenced cells as measured by a focus-forming assay. The viral yield was not significantly changed by silencing PKG.

Western blot analysis, and total PKG activity (Fig. 10A and B) at both 48 and 96 h. Cells were infected 48 h after either mock transfection or transfection of PKG Iα/β siRNA or scrambled siRNA, and the viral yields were measured 48 h after infection. DENV replication in the PKG-silenced cells was ~2 logs lower than that in the scrambled RNA control cells (P value, <0.00001; Fig. 10C), while LGTV was not affected (Fig. 10D). These results suggest that PKG activity modulates mosquito-borne flaviviral replication in human cells but not tick-borne flaviviral replication.

DISCUSSION

In this report, we mapped a potential serine/threonine flaviviral phosphorylation site that is conserved in two different mosquito-borne viruses, DENV and YFV. Furthermore, we

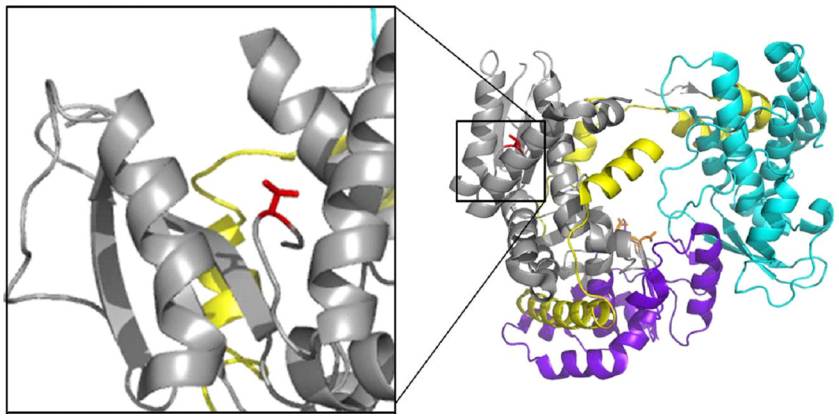

FIG. 11. Structure of DENV-3 polymerase domain, with T449 highlighted. The DENV-3 RNA polymerase (residues 273 to 896) structure was used to map the DENV-2 threonine 449. The corresponding residue in DENV-3 is a serine which has been changed to a threonine (red) in this representation. The finger, palm, and thumb subdomains of the RdRP are colored gray, purple, and cyan, respectively. The nuclear localization sequence regions are shown in yellow, and the conserved aspartate residues involved in the catalytic reaction (motif C) are shown as stick representations in orange, while the site of catalysis is indicated with an orange asterisk. An enlarged view of the region around T449 shows that the residue is located on a loop with a solvent-exposed side chain. This location indicates that the threonine side chain could be accessible to the cellular kinase during the phosphorylation reaction, and significant movement between the subdomains during polymerization could either expose or make the residue inaccessible for phosphorylation. T449 is far removed from the site of polymerization, making its direct contribution to the enzymatic reaction unlikely.

show that this specific site of NS5 can be phosphorylated by cGMP-dependent PKG in vitro. While the first suggestion that this phosphorylation site was recognized by PKG came from a neural net bioinformatics program, it is noteworthy that this viral site differs from the well-described RKRKXST motif of the canonical PKG substrates (20). Since the PKG signaling pathway regulates a variety of physiological processes in many different cell types, it is likely that not all the recognition sites are known.

Three enzymes mediate cGMP-dependent kinase activity in mammalian cells. They are produced from two genes, cGKI (which produces PKG Iα and PKG Iβ) and cGKII (which produces PKG II). The enzymes from these genes differ in their tissue distributions, subcellular localizations, and substrates. At least in vitro, all three are able to phosphorylate DENV NS5, even though in vivo they have different substrates and regulate a diverse range of physiological functions, including learning, circadian rhythm, phototaxis, vascular tone, kidney function, platelet aggregation, and intestinal secretion (20). The pharmacologic data presented here suggest that modulation of PKG activity alters DENV replication. The phosphoacceptor motif described above is conserved in all four serotypes of DENV, YFV, WNV, and Japanese encephalitis virus, as well all other flaviviruses known to be transmitted by mosquitoes, but not the tick-borne flaviviruses (Fig. 7). A threonine-to-serine variation is common at position 449 in DENV isolates, particularly in DENV-3 and DENV-4. Based on the crystal structure of DENV-3 NS5 (Fig. 11), the residue 449 site is solvent exposed and is likely accessible to a kinase. Mosquito-borne flaviviruses have diverged in their evolution to have a serine or threonine phosphoacceptor site at this position, unlike other flaviviruses. Whether there are additional properties besides phosphorylation that make a threonine/serine requirement is unclear at present. When purified full-length DENV NS5 was phosphorylated in vitro with PKG Iα and the polymerase activity was compared to nonphosphorylated protein, no enhancement or inhibition of activity was observed (data not shown). Our evidence suggests that a transient phosphorylation at residue 449 on a threonine is tolerated by DENV replication, but placement of a nonreversible negative charge, such as the glutamic acid at residue 449, is detrimental to genome replication. A histidine is also not tolerated in replication, even though it is the observed residue in tick-borne flaviviruses.

Currently, we have evidence only that cGMP-dependent pathways alter DENV replication in mammalian cells, and there are no published data on PKG activity in mosquitoes. PKG activity is known to exist in drosophilae and honey bees. It is noteworthy, though, that PKG activity has been linked to behavior in a wide variety of organisms, including mammals and insects (19). For drosophilae (15) and honey bees (1), both genetic and pharmacologic data have linked PKG activity to insect foraging behavior. While the idea is speculative, there may be evolutionary advantages for viruses transmitted by mosquitoes to encode PKG substrates that have little to do with viral replication in cell culture. It is unclear if the phosphoacceptor is conserved for virus replication reasons or other attributes required for the virus to be evolutionarily successful.

In conclusion, DENV, like YFV, has a number of usable phosphoacceptor sites consistent with a hyperphosphorylated form in viral infection (2, 9). Surprisingly, only one of these sites was found in both YFV and DENV. Other sites could be phosphorylated in both because we were not able to detect peptides covering the entire protein for either viral protein. While phosphorylation of serines and threonines of NS5 is known to occur in both mosquito-borne (9, 11) and tick-borne (13) flaviviruses, this residue is specifically conserved for flaviviruses transmitted by mosquitoes. This site is phosphorylated by cGMP-activated PKG in a cell-free assay. Replacement of threonine with the tick-specific residue is detrimental to DENV replication. Modulations of the cGMP pathway, such as either activation or inhibition of PKG, alter DENV repli-

cation but not LGTV replication, which lacks the homologous PKG phosphoacceptor site. To our knowledge, this is the first linkage between PKG activity and flavivirus replication. Additional research on the interaction between mosquito-borne flaviviruses and the PKG pathway is warranted.

ACKNOWLEDGMENTS

This work was sponsored by the NIH/NIAID Regional Center of Excellence for Biodefense and Emerging Infectious Diseases Research (RCE) program. We acknowledge membership within and support from the Region V Great Lakes RCE program (NIH award 1-U54-AI-057153) as well as support by a Public Health Service Program Project grant (AI55672) from the National Institute of Allergy and Infectious Diseases to R.K. We thank the University of Wisconsin—Madison Biotechnology mass spectrometry facility and the Human Proteomics Mass Spectrometry Facility, supported by the The Wisconsin Partnership Fund for a Healthy Future, for technical assistance.

We also thank James Wolfinbarger for the doing the LGTV focus-forming assays.

REFERENCES

1. **Ben-Shahar, Y., A. Robichon, M. B. Sokolowski, and G. E. Robinson.** 2002. Influence of gene action across different time scales on behavior. Science **296:**741–744.
2. **Bhattacharya, D., S. Hoover, S. P. Falk, B. Weisblum, M. Vestling, and R. Striker.** 2008. Phosphorylation of yellow fever virus NS5 alters methyltransferase activity. Virology **380:**276–284.
3. **Black, T. M., C. L. Andrews, G. Kilili, M. Ivan, P. N. Tsichlis, and P. Vouros.** 2007. Characterization of phosphorylation sites on Tpl2 using IMAC enrichment and a linear ion trap mass spectrometer. J. Proteome Res. **6:**2269–2276.
4. **Blom, N., T. Sicheritz-Ponten, R. Gupta, S. Gammeltoft, and S. Brunak.** 2004. Prediction of post-translational glycosylation and phosphorylation of proteins from the amino acid sequence. Proteomics **4:**1633–1649.
5. **Crooks, G. E., G. Hon, J. M. Chandonia, and S. E. Brenner.** 2004. WebLogo: a sequence logo generator. Genome Res. **14:**1188–1190.
6. **Forwood, J. K., A. Brooks, L. J. Briggs, C. Y. Xiao, D. A. Jans, and S. G. Vasudevan.** 1999. The 37-amino-acid interdomain of dengue virus NS5 protein contains a functional NLS and inhibitory CK2 site. Biochem. Biophys. Res. Commun. **257:**731–737.
7. **Gould, E. A., and T. Solomon.** 2008. Pathogenic flaviviruses. Lancet **371:**500–509.
8. **Ho, S. N., H. D. Hunt, R. M. Horton, J. K. Pullen, and L. R. Pease.** 1989. Site-directed mutagenesis by overlap extension using the polymerase chain reaction. Gene **77:**51–59.
9. **Kapoor, M., L. Zhang, M. Ramachandra, J. Kusukawa, K. E. Ebner, and R. Padmanabhan.** 1995. Association between NS3 and NS5 proteins of dengue virus type 2 in the putative RNA replicase is linked to differential phosphorylation of NS5. J. Biol. Chem. **270:**19100–19106.
10. **Kim, S. J., J. H. Kim, Y. G. Kim, H. S. Lim, and J. W. Oh.** 2004. Protein kinase C-related kinase 2 regulates hepatitis C virus RNA polymerase function by phosphorylation. J. Biol. Chem. **279:**50031–50041.
11. **Mackenzie, J. M., M. T. Kenney, and E. G. Westaway.** 2007. West Nile virus strain Kunjin NS5 polymerase is a phosphoprotein localized at the cytoplasmic site of viral RNA synthesis. J. Gen. Virol. **88:**1163–1168.
12. **Mitzel, D. N., S. M. Best, M. F. Masnick, S. F. Porcella, J. B. Wolfinbarger, and M. E. Bloom.** 2008. Identification of genetic determinants of a tick-borne flavivirus associated with host-specific adaptation and pathogenicity. Virology **381:**268–276.
13. **Morozova, O. V., N. A. Tsekhanovskaya, T. G. Maksimova, V. N. Bachvalova, V. A. Matveeva, and Y. Kit.** 1997. Phosphorylation of tick-borne encephalitis virus NS5 protein. Virus Res. **49:**9–15.
14. **Neddermann, P., M. Quintavalle, C. Di Pietro, A. Clementi, M. Cerretani, S. Altamura, L. Bartholomew, and R. De Francesco.** 2004. Reduction of hepatitis C virus NS5A hyperphosphorylation by selective inhibition of cellular kinases activates viral RNA replication in cell culture. J. Virol. **78:**13306–13314.
15. **Osborne, K. A., A. Robichon, E. Burgess, S. Butland, R. A. Shaw, A. Coulthard, H. S. Pereira, R. J. Greenspan, and M. B. Sokolowski.** 1997. Natural behavior polymorphism due to a cGMP-dependent protein kinase of Drosophila. Science **277:**834–836.
16. **Payne, A. F., I. Binduga-Gajewska, E. B. Kauffman, and L. D. Kramer.** 2006. Quantitation of flaviviruses by fluorescent focus assay. J. Virol. Methods **134:**183–189.
17. **Pryor, M. J., S. M. Rawlinson, R. E. Butcher, C. L. Barton, T. A. Waterhouse, S. G. Vasudevan, P. G. Bardin, P. J. Wright, D. A. Jans, and A. D. Davidson.** 2007. Nuclear localization of dengue virus nonstructural protein 5 through its importin alpha/beta-recognized nuclear localization sequences is integral to viral infection. Traffic **8:**795–807.
18. **Quintavalle, M., S. Sambucini, V. Summa, L. Orsatti, F. Talamo, R. De Francesco, and P. Neddermann.** 2007. Hepatitis C virus NS5A is a direct substrate of casein kinase I-alpha, a cellular kinase identified by inhibitor affinity chromatography using specific NS5A hyperphosphorylation inhibitors. J. Biol. Chem. **282:**5536–5544.
19. **Reed, K. E., A. E. Gorbalenya, and C. M. Rice.** 1998. The NS5A/NS5 proteins of viruses from three genera of the family *Flaviviridae* are phosphorylated by associated serine/threonine kinases. J. Virol. **72:**6199–6206.
20. **Schlossmann, J., and F. Hofmann.** 2005. cGMP-dependent protein kinases in drug discovery. Drug Discov. Today **10:**627–634.
21. **Selisko, B., H. Dutartre, J. C. Guillemot, C. Debarnot, D. Benarroch, A. Khromykh, P. Desprès, M. P. Egloff, and B. Canard.** 2006. Comparative mechanistic studies of de novo RNA synthesis by flavivirus RNA-dependent RNA polymerases. Virology **351:**145–158.
22. **Smith, J. A., R. B. Reed, S. H. Francis, K. Grimes, and J. D. Corbin.** 2000. Distinguishing the roles of the two different cGMP-binding sites for modulating phosphorylation of exogenous substrate (heterophosphorylation) and autophosphorylation of cGMP-dependent protein kinase. J. Biol. Chem. **275:**154–158.
23. **Tellinghuisen, T. L., K. L. Foss, and J. Treadaway.** 2008. Regulation of hepatitis C virion production via phosphorylation of the NS5A protein. PLoS Pathog. **4:**e1000032.
24. **World Health Organization.** 2002. Dengue factsheet. World Health Organization, Geneva, Switzerland.